Applied Physics A (2020) 126:133
https://doi.org/10.1007/s00339-020-3316-z

Applied Physics A
Materials Science & Processing

Structural and mechanical properties of amorphous $AlMgB_{14}$ thin films deposited by DC magnetron sputtering on Si, Al_2O_3 and MgO substrates

Mohammad Noroozi[1,2] · Andrejs Petruhins[1] · Grzegorz Greczynski[1] · Johanna Rosen[1] · Per Eklund[1]

Received: 21 May 2018 / Accepted: 14 January 2020 / Published online: 28 January 2020

Abstract

$AlMgB_{14}$ coatings have been deposited by DC magnetron sputtering from elemental targets on Si (001), Al_2O_3 (0001) and MgO (001) substrates at temperatures in the range of 25–350 °C. The structural and mechanical properties of $AlMgB_{14}$ films were characterized by X-ray diffraction, scanning electron microscopy, nanoindentation, and analyzed as a function of deposition conditions and substrate materials. The results show that all films are X-ray amorphous, and the mechanical properties of the deposited films depend on the substrate and growth temperature. $AlMgB_{14}$ thin films deposited at 350 °C are found to have smoother surfaces and containing more well-formed B_{12} icosahedra than the films deposited at lower temperature, which consequently increase the hardness of the deposited films. The maximum hardness and Young's modulus of the as-deposited films are about 32.3 GPa and 310 GPa, respectively, for films deposited on Al_2O_3 substrate at 350 °C.

Keywords Boride · Physical vapor deposition · Nanoindentation · Sputter-deposition · X-ray diffraction

1 Introduction

Boron-rich solids are materials with boron as their primary atomic component. The crystal structures of many high-boron-content compounds contain B_{12} icosahedra based on 12-atom clusters in which atoms occupy the 12 vertices of an icosahedron [1]. These dense B networks with unusual bonding generates interesting mechanical and transport properties. Hardness values range from 30 to 50 GPa [2, 3], bulk moduli from 196 to 235 GPa [4–6] and melting points up to 2400 °C, underlining the exceptional bond strength of these B-networks [1]. The ternary boride $AlMgB_{14}$ is one of the promising boron-rich boride materials that can form icosahedral structures and has been investigated intensively during last years. This material is attractive due to high hardness, low density, high thermal stability and interesting thermoelectric properties [7, 8].

The formation of B icosahedra can occur both in amorphous B compound from icosahedral bonding features (not to be confused with icosahedral crystal structures, i.e. some quasicrystals) and in crystalline B structures [9, 10]. Tian et al. reported that icosahedra partially formed at room temperature [11], and suggested that deposition at temperatures between 200 and 350 °C can facilitate the formation of icosahedral features [11]. Therefore, it is desirable to study the effect of deposition of $AlMgB_{14}$ thin film at substrate temperatures close to possible formation of B_{12} icosahedra framework. Up to now, $AlMgB_{14}$ in bulk or powder form has been prepared by several methods like mechanical alloying, hot pressing and pulsed electric current sintering [7, 12]. Although most efforts have been focused on preparing $AlMgB_{14}$ in bulk or powder form, a few reports have shown preparation as thin films [2, 4, 13–17], primarily using pulsed laser deposition (PLD). Limited attempts on preparation by magnetron sputtering have been done. Preparation with magnetron sputtering is desirable over PLD since sputter-deposition is a more established technique and allows for process control and ease of upscaling. Furthermore, deposition of complex form of hard coating tools or deposition on large substrates is easier than PLD [2].

✉ Per Eklund
per.eklund@liu.se

Mohammad Noroozi
adrinnoroozi@hotmail.com

1 Thin Film Physics Division, Department of Physics, Chemistry, and Biology (IFM), Linköping University, 581 83 Linköping, Sweden

2 Present Address: Finisar Sweden AB, 175 27 Järfälla, Sweden

In most studies, $AlMgB_{14}$ was prepared on Si substrates, while, for example, in thermoelectric devices, to avoid thermal and electrical leakage through the substrate, the device layer is preferred to be on the insulator. Therefore, deposition on lower thermal conductivity materials in comparison to Si, like Al_2O_3 and MgO substrates [18–20] can be preferable for some applications. In this study, we synthesize ternary boride $AlMgB_{14}$ films by DC magnetron sputtering with a three-target magnetron sputtering system on Si (001), Al_2O_3 (0001) and MgO (001) substrates at temperature range of 25–350 °C.

2 Materials and methods

To deposit thin films, an ultrahigh vacuum chamber with a base pressure of 3.5×10^{-7} Pa have been used. B, Al and Mg elemental magnetron sputtering targets were mounted at a distance (from target center to substrate) of 180 mm for Mg, B and 150 mm for Al. The deposition system and geometry are described in detail elsewhere [19, 21]. The deposition was carried out on an MgO (001), Al_2O_3 (0001) and Si (001) substrates at temperatures of 25, 250 and 350 °C. All substrates were cleaned in acetone and isopropanol for 5 min each and finally native oxide was removed from Si substrates using HF 0.5% to ensure Si surfaces are identical. Finally, all substrates were blown-dried by nitrogen gas and then placed into the vacuum chamber immediately. Prior to the deposition, Ar gas, whose flow rate can be regulated by mass flow controller, was introduced into the chamber where a total pressure was maintained at 0.53 Pa during deposition. To keep uniformity during deposition, substrates were rotated at 5 rpm. Prior to the actual film deposition, targets were run for 10 min behind shutters to clean the targets and reach steady-state condition. To find $AlMgB_{14}$ thin film with the required stoichiometric composition in each temperature, the B, Mg and Al target sputtering powers were tuned until reaching the desired composition. The deposition parameters for final samples after optimization near the desired stoichiometry are listed in Table 1.

Atomic-force microscope (AFM) and scanning electron microscope (SEM) were used to investigate surface topology and roughness. X-ray photoelectron spectroscopy (XPS) analyses were performed with AXIS Ultra DLD instrument from Kratos Analytical (UK) with base pressure during spectra acquisition lower than 1.3×10^{-7} Pa and employing monochromatic Al Kα (1486.6 eV) radiation. Samples were analyzed in the as-received state as well as after sputter-cleaning to remove adsorbed contaminants following air exposure. The cleaning procedure consisted of two steps: first 4 keV Ar^+ ion beam incident at an angle of 20° from the surface and rastered over the area of 3×3 mm^2 was used for 2 min. After that, the Ar^+ ion energy was reduced to 0.5 keV for the final cleaning which lasted for 10 min. The binding energy scale was calibrated according to the procedure described in Ref. [22] for as-received samples. Quantification of the XPS core-level spectra was performed using Casa XPS software (version 2.3.16) and elemental sensitivity factors supplied by Kratos Analytical Ltd. The error bars for XPS-determined element concentrations are around ± 5%. Nanoindentation was carried out using a Hysitron TriboIndenter with a Berkovich diamond tip with load peaking of 1000 µN. The tip area function was calibrated on a fused-silica sample and each sample was measured 15 times to get a statistically valid average value. The hardness (H) and reduced elastic modulus E_r were calculated by the method of Oliver and Pharr using the unloading elastic part of the load-displacement curve. The structure of deposited films was investigated by X-ray diffraction (XRD) and finally, the local bonding information was extracted by Fourier-transform infrared spectroscopy (FTIR). FTIR spectra were obtained with a Bruker Vertex 70 spectrometer using the KBr pellet method; the system was continuously purged with nitrogen before and during the measurements. All spectra were acquired at 2 cm^{-1} resolutions with a total of 200 scans, and over a wavenumber range between 600 and 5000 c^{-1}.

3 Results and discussion

The elemental composition of $AlMgB_{14}$ thin films was characterized by XPS. First, it was confirmed that the Al, Mg and B elements from three targets are all present in the films. Figure 1a and b shows Al 2p, Mg 2 s, and B1s XPS

Table 1 Deposition parameters of $AlMgB_{14}$ thin films

Base pressure 3.5×10^{-7} Pa
Working pressure 1.1×10^{-1} Pa
Ar flow rate 71 sccm
Deposition time 3 h (deposition rate ~ 2 nm/min; film thickness ~ 360 nm)
DC power of Mg target 5 W (at T: 25 ℃), 40 W (at T: 250 ℃, 90 W (at T: 350 ℃)
DC power of Al target 3 W (at T: 25 and 250 ℃), 5 W (at T: 350 ℃)
DC power of B target 300 W (at T: 25, 250 and 350 ℃)
Substrate temperature 25, 250, 350 ℃

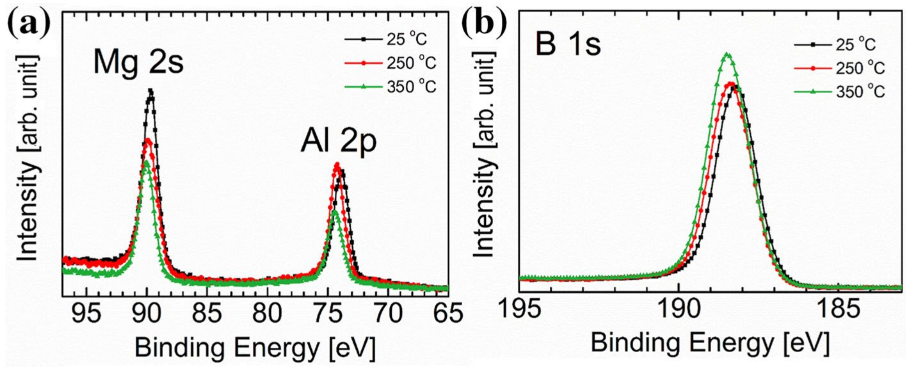

Fig. 1 XPS spectra of $AlMgB_{14}$ films deposited at 25 °C, 250 °C, and 350 °C

Table 2 Composition determined by XPS on Si substrate

	Temperature °C	B at%	Mg at%	Al at%	O at%
Sample 1	25	82	7.5	7.5	3
Sample 2	250	84	6.5	7.5	2
Sample 3	350	89	4.5	4.5	2
Ideal $AlMgB_{14}$ composition		90	5	5	–

spectra obtained from samples grown at different temperatures. All core levels exhibit a minor shift of 0.2–0.3 eV towards higher binding energy (BE) with increasing temperature. The BE of the Al 2p peak, in the range 74.0 (25 ℃)–74.3 eV (350 ℃) shows that Al is in the sub-stoichiometric oxide regime, as both metallic Al and Al-B bonds appear at significantly lower BE. B1s signal is present at the BE of 188.2–188.4 eV, which is in the range typical for B–B [23]or B–metal bond, [24] and definitely lower than that of B–O (typically at 192–193 eV) [24]. A relatively large full width at half maximum of 1.7–1.8 eV, may indicate multiple chemical states. The BE of the Mg 2 s peaks is in the range 89.7–90.0 eV, which is somewhat higher than 89.0 eV expected for metallic Mg [23] which could indicate Mg–B or Mg–O formation.

The XPS-derived film compositions for sputter-cleaned samples are listed in Table 2. The Mg content was estimated based on the Mg 2 s rather than commonly used Mg 1 s core-level peak to ensure that photoelectron kinetic energy is closer to that of Al 2p and B 1 s electrons which should result in similar probing depth, and hence, more reliable quantification. It can be observed that with increasing growth temperature T the boron content increases from 82 at % in sample 1 with $T = 25$ °C to 89 at % in sample 3 with $T = 350$ °C. This is accompanied by decrease in both Al and Mg concentration from 7.5 at % with $T = 25$ ℃ to 4.5 at % for both Al and Mg with $T = 350$ °C. Thus, the substrate temperature affects the composition of as-deposited films in that the Mg (and Al) content decreases at higher substrate temperatures. Since Mg has a high vapor pressure over a broad temperature range, this is expected. The residual O originates from native oxide, post-deposition incorporation when exposed to air and redeposited in UHV during measurement and/or implanted during Ar^+ cleaning step. For all as-deposited $AlMgB_{14}$ thin films, the oxygen content is in the range of 2–3 at.%. The oxygen content is likely underestimated due to the fact that electrons originating from the O 1 s core level have substantially shorter mean free paths on the way to the surface than those from the Al 2p level. The difference is caused by difference in the kinetic energy, which is 950 and 1410 eV for O 1 s and Al 2p electrons, respectively.

Figure 2 shows the θ–2θ XRD patterns of the films deposited at 25, 250 and 350 °C on different substrates. The as-deposited films are all X-ray amorphous regardless of deposition temperature and substrate types. All observed Bragg reflexes are the substrate peaks for Si, Al_2O_3 and MgO. It can, therefore, be concluded that crystalline $AlMgB_{14}$ phase is not obtained at these deposition temperatures.

Figure 3a shows an SEM micrograph of sample 1. SEM shows segregated islands on the surface. Figure 3b shows a line mapping EDX analysis of one large island on this sample to check composition variation. The EDX result shows that this composition changed marginally in the island area and there is no evidence of segregation of any of the elements individually.

To obtain smooth surfaces without islands at room temperature, the processing conditions was adjusted using a negative bias voltage (− 200 V) and by increasing the target-to-substrate distance from 15 to 22 cm. As shown in the SEM surface image in Fig. 3c, longer distance between substrate and target decrease formation of islands and improve quality of surface. The surface of the sample in Fig. 3d, deposited using − 200 V as bias voltage, has no segregation and exhibits a homogeneous and smooth surface, i.e., the ion bombardments causes an increased density and smoothens the surface of the films compared to the sample without bias.

To investigate the possibility of formation of icosahedral bonding features in the boride films, FTIR

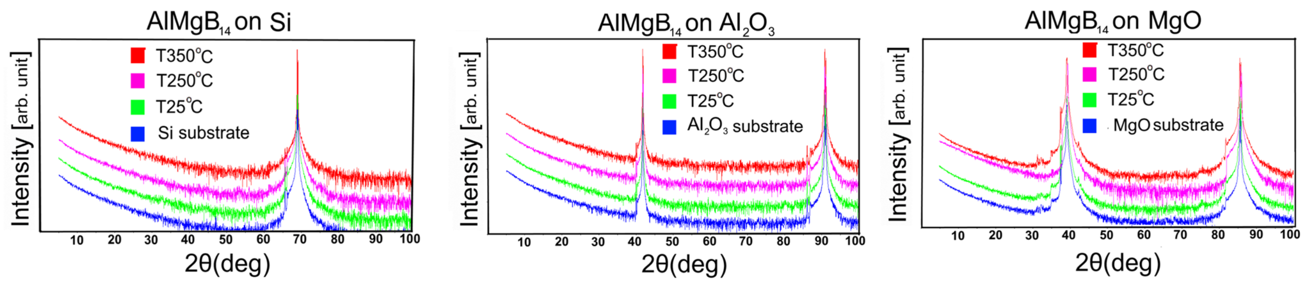

Fig. 2 XRD patterns of $AlMgB_{14}$ thin film on Si, Al_2O_3 (0001), and MgO (111)

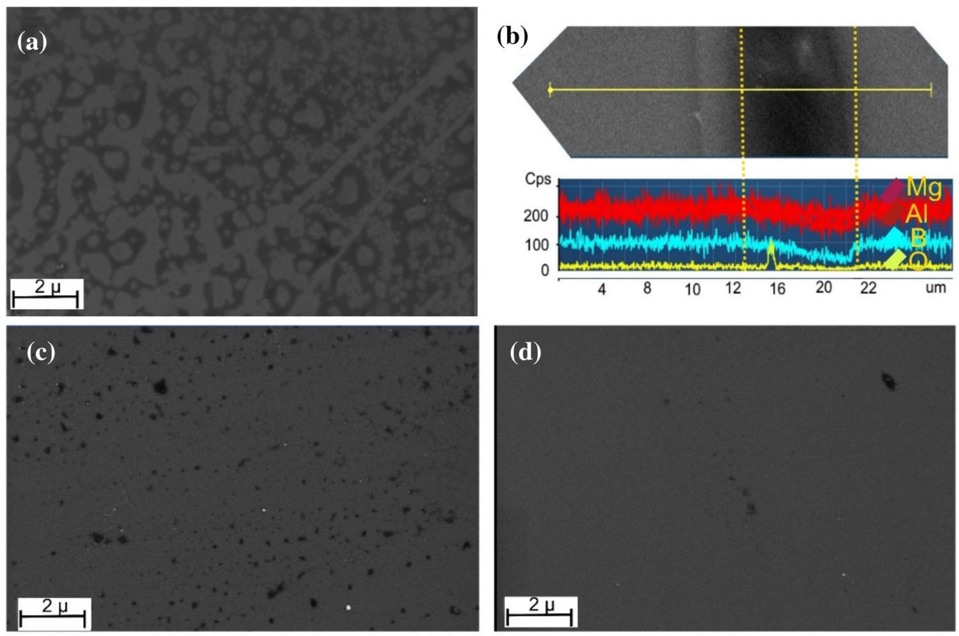

Fig. 3 SEM images **a** as-deposited $AlMgB_{14}$ at 25 °C on Si, **b** EDX analysis on semi-segregated areas on sample 1, **c** as-deposited $AlMgB_{14}$ at 25 °C on Si, 7 cm longer distance from target, **d** as-deposited $AlMgB_{14}$ at 25 ℃ on Si substrate of −200 V

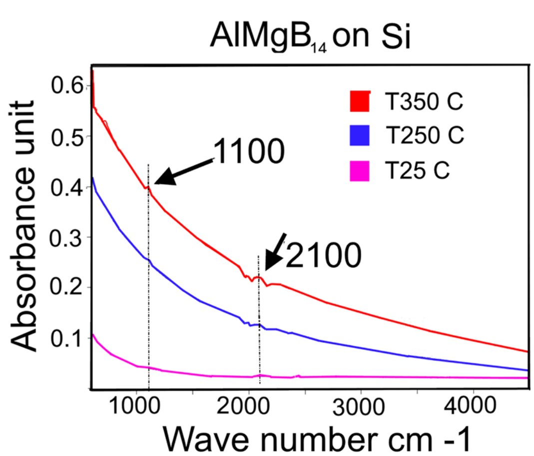

Fig. 4 FTIR spectra of $AlMgB_{14}$ thin films on Si substrate

measurements of $AlMgB_{14}$ thin films deposited at 25, 250 and 350 °C (sample 1–3) was carried out. The results are shown in Fig. 4. The spectra exhibit two absorption peaks near 1100 cm^{-1} and 2100 cm^{-1}, which are attributed to the vibrational mode of a single B_{12} icosahedron. The intra-icosahedral vibrations are localized in the range of 800 cm^{-1}, whereas the inter-icosahedral vibrations appear at higher wave numbers [25].The amorphization leads to an enhancement of the vibrations in the range of 1100–1250 cm^{-1} [25]. Here, the FTIR data indicate the presence of B_{12} icosahedra in the amorphous $AlMgB_{14}$. The low absorption intensity at 25 and 250 °C indicates that the B_{12} icosahedra were not fully developed at low temperatures but suggests that the higher substrate temperature enables the formation of B_{12} icosahedra. This, together with the FTIR results, indicates the formation of amorphous $AlMgB_{14}$ with local icosahedral features at 350 °C.

To study the mechanical properties of the thin films, nanoindentation was used. The indentation depth was kept around 10% of the film thickness (360 nm) to avoid substrate effects. Fifteen indents were made in each sample. The load-displacement curves are shown in Fig. 5. The results are the

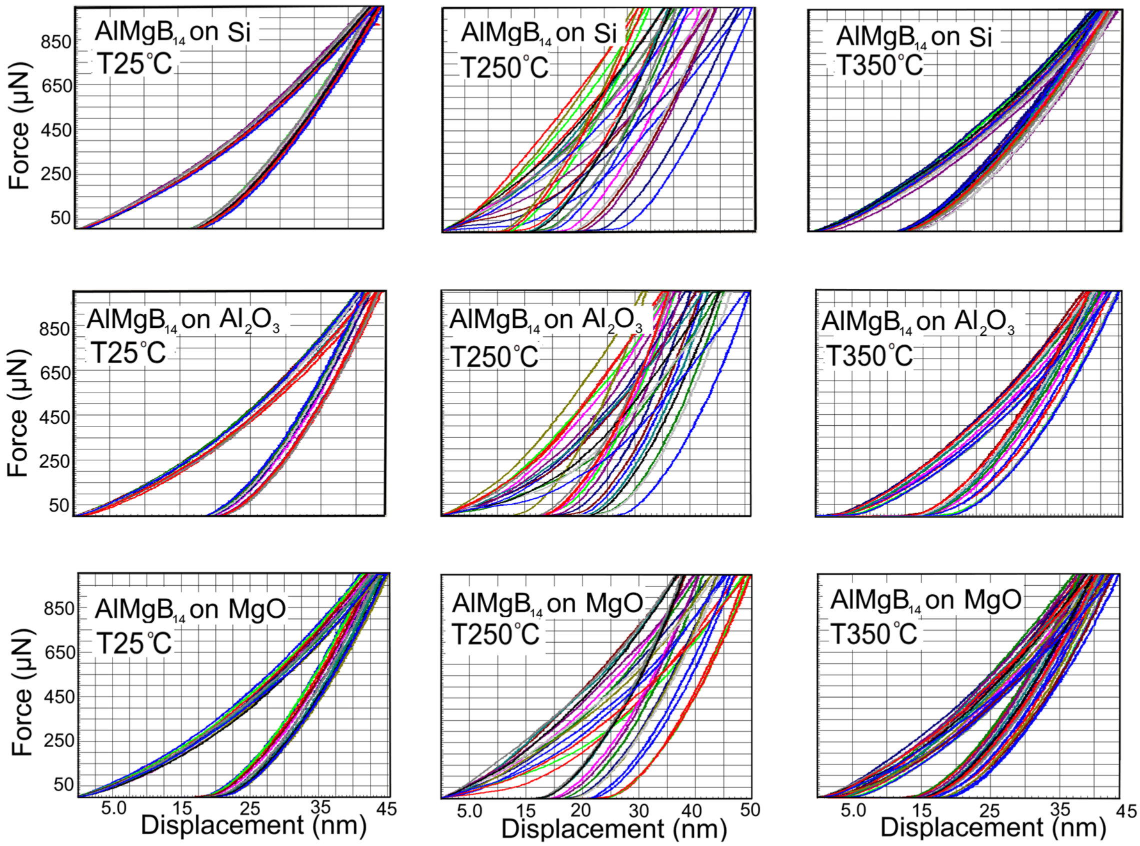

Fig. 5 Load-displacement curves for $AlMgB_{14}$ thin films

average of these indentations for the hardness and reduced Young's modulus, summarized in Table 3.

The curves in Fig. 5 show the measured hardness of the films have an almost constant value for temperature 25 and 350 °C but more scattered for the film deposited at 250 °C. This scattering is expected as a consequence of rougher surfaces. The minimum values for hardness and Young's modulus was measured for samples deposited at 250 °C, whereas the maximum values are exhibited in samples deposited at 350 °C with the peak of hardness (32.3 ± 1.7 GPa) and Young's modulus (310 ± 6 GPa) by $AlMgB_{14}/Al_2O_3$. A plausible explanation for observing higher hardness at 350 °C on Al_2O_3 substrate may be the lower thermal conductivity of Al_2O_3, in comparison to Si,

Table 3 Hardness H, reduced Young's modulus E_r and roughness in $AlMgB_{14}$ (the stated error bars correspond to the standard deviations)

	Temperature °C	Substrate	Hardness H (GPa)	Young's modulus E_r (GPa)
T1	25	Si	23.2 ± 1	222 ± 4
T2	250	Si	20.5 ± 4	188 ± 23
T3	350	Si	29.5 ± 1	243 ± 6
T4	25	Al_2O_3	22.3 ± 1	280 ± 5
T5	250	Al_2O_3	21.3 ± 5	299 ± 27
T6	350	Al_2O_3	32.3 ± 2	310 ± 6
T7	25	MgO	21.8 ± 1	259 ± 7
T8	250	MgO	21.4 ± 3	254 ± 31
T9	350	MgO	26.4 ± 2	279 ± 17
T10	25	Si (different target to substrate distance: 22 cm)	25.3 ± 1	211 ± 4
T11	25	Si (bias voltage − 200 V)	21 ± 1	208 ± 3

which results in more stable temperature and denser microstructure during sputtering at 350 °C temperature. Hardness and Young's modulus values are comparable to other reports about $AlMgB_{14}$ as hard coating material [5, 11, 14].

4 Conclusions

We have grown $AlMgB_{14}$ thin films on Si (001), MgO (001) and Al_2O_3 (0001) substrates using three elemental targets in DC magnetron sputtering at 25, 250 and 350 °C. XPS results indicate that the O content is kept under 3% in all samples. For increased substrate temperature (350 °C), the film composition is closer to ideal $AlMgB_{14}$. The hardness and reduced Young's modules of samples are more dependent on temperature which may be due to formation of icosahedral bonding features.

Acknowledgements Open access funding provided by Linköping University. The authors acknowledge the Knut and Alice Wallenberg Foundation for Project Grant KAW 2015.0043 and the Academy Fellows program. GG acknowledges support from Knut and Alice Wallenberg Foundation Scholar Grant KAW 2016.0358, the Åforsk Foundation Grant 16-359, and Carl Tryggers Stiftelse contract CTS 17:166.

References

1. D. Emin, Unusual properties of icosahedral boron-rich solids. J. Solid State Chem. **179**, 2791–2798 (2006)
2. M.H. Yuzvyuk, V.V. Putrolaynen, A.M. Grishin, Processing of ultra-hard coatings based on AlMgB $_{14}$ films. J. Phys. Conf. Ser. **769**, 12039 (2016)
3. Y. Tian, G. Li, J. Shinar et al., Electrical transport in amorphous semiconducting $AlMgB_{14}$ films. Appl. Phys. Lett. **85**, 1181 (2004)
4. A.M. Grishin, S.I. Khartsev, J. Böhlmark, M. Ahlgren, Ultra-hard $AlMgB_{14}$ coatings fabricated by RF magnetron sputtering from a stoichiometric target. JETP Lett. **100**, 766–773 (2014)
5. A.M. Grishin, V.V. Putrolaynen, M.H. Yuzvyuk, Ultra-hard amorphous $AlMgB_{14}$ films RF sputtered onto curved substrates. Mater. Res. Express **4**, 36406 (2017)
6. A.M. Grishin, films Abrasion resistant low friction and ultra-hard magnetron sputtered. Mater. Res. Express **3**, 46402 (2016)
7. M. Takeda, T. Fukuda, F. Domingo, T. Miura, Thermoelectric properties of some metal borides. J. Solid State Chem. **177**, 471–475 (2004)
8. I. Bairamashvili, L. Kekelidze, O. Golikova, The preparation of α-AlB_{12} and $AlMgB_{14}$ samples and an investigation of their electrothermal properties. J. Less Common Metal **67**, 461–464 (1979)
9. K.Y. Xie, Q. An, T. Sato et al., Breaking the icosahedra in boron carbide. Proc. Natl. Acad. Sci. **113**, 12012–12016 (2016)
10. R. Schmechel, H. Werheit, On the dynamical conductivity in icosahedral boron-rich solids. J. Phys. Condens. Matter **8**, 7263–7275 (1996)
11. Y. Tian, A.F. Bastawros, C.C.H. Lo et al., Superhard self-lubricating $AlMgB_{14}$ films for microelectromechanical devices. Appl. Phys. Lett. **83**, 2781–2783 (2003)
12. Y. Tian, A. Constant, C.C.H. Lo et al., Microstructure evolution of Al–Mg–B thin films by thermal annealing. J. Vac. Sci. Technol. A Vac. Surf. Film **21**, 1055–1063 (2003)
13. C.S. Li, F. Yang, G. Yan et al., $AlMgB_{14}$–TiB_2 synthesized by a two-step heat-treatment method. J. Alloys Compd. **587**, 790–793 (2014)
14. Z. Wu, Y. Bai, W. Qu et al., Al–Mg–B thin films prepared by magnetron sputtering. Vacuum **85**, 541–545 (2010)
15. S. Jing, Y. Bai, F. Qin, J. Xiao, Bias effects on AlMgB thin films prepared by magnetron sputtering. Surf. Eng. **33**, 592–596 (2017)
16. Y. Tian, Deposition and characterization of $AlMgB_{14}$ thin film coatings. PhD thesis: Iowa State University (2004)
17. H. Kölpin, D. Music, G. Henkelman et al., Phase stability of $AlYB_{14}$ sputtered thin films. J. Phys. Condens. Matter (2009). https://doi.org/10.1088/0953-8984/21/35/355006
18. L.D. Madsen, R. Charavel, J. Birch, E.B. Svedberg, Assessment of MgO (1 0 0) and (1 1 1) substrate quality by X-ray diffraction. J. Cryst. Growth **209**, 91 (2000)
19. A.L. Febvrier, J. Jensen, P. Eklund, Wet-cleaning of MgO (001): Modification of surface chemistry and effects on thin film growth investigated by X-ray photoelectron spectroscopy and time-of-flight secondary ion mass spectroscopy. Vac. Sci. Technol. A Vac. Surf. Film **35**, 21407 (2017)
20. J.L. Schroeder, A.S. Ingason, J. Rosén, J. Birch, Beware of poor-quality MgO substrates: a study of MgO substrate quality and its effect on thin film quality. Cryst. Growth **420**, 22–31 (2015)
21. J. Emmerlich, H. Högberg, S. Sasvári et al., Growth of Ti_3SiC_2 thin films by elemental target magnetron sputtering. J. Appl. Phys. **96**, 4817–4826 (2004)
22. G. Greczynski, L. Hultman, C 1s peak of adventitious carbon aligns to the vacuum level: dire consequences for material's bonding assignment by photoelectron spectroscopy. ChemPhysChem **18**, 1507–1512 (2017)
23. J.F. Moulder, W.F. Stickle, P.E. Sobol, *Handbook of X-ray photoelectron spectroscopy* (Perkin-Elmer Corporation, Eden Prairie, 1992)
24. L. Tengdelius, G. Greczynski, M. Chubarov et al., Stoichiometric, epitaxial ZrB_2 thin films with low oxygen-content deposited by magnetron sputtering from a compound target: effects of deposition temperature and sputtering power. J. Cryst. Growth **430**, 55–62 (2015)
25. V.I. Ivashchenko, P.E.A. Turchi, S. Veprek et al., First-principles study of crystalline and amorphous $AlMgB_{14}$-based materials. J. Appl. Phys. **119**, 205105 (2016)